RISING: Gamma-ray Spectroscopy with Radioactive Beams at GSI

P. Doornenbal[a,b], A. Bürger[c], D. Rudolph[d], H. Grawe[b], H. Hübel[c], P.H. Regan[e], P. Reiter[a], A. Banu[b], T. Beck[b], F. Becker[b], P. Bednarczyk[b,f], L. Caceres[b,g], H. Geissel[b], J. Gerl[b], M. Górska[b], J. Grębosz[b,f], M. Kavatsyuk[b], O. Kavatsyuk[b], A. Kelic[b], I. Kojouharov[b], N. Kurz[b], R. Lozeva[b,h], F. Montes[b], W. Prokopowicz[b], N. Saito[b], T. Saito[b], H. Schaffner[b], S. Tashenov[b], H. Weick[b], E. Werner-Malento[b,i], M. Winkler[b], H.-J. Wollersheim[b], A. Al-Khatib[c], L.-L. Andersson[d], L. Atanasova[h], D.L. Balabanski[j], M.A. Bentley[k], G. Benzoni[l], A. Blazhev[a], A. Bracco[l], S. Brambilla[l], C. Brandau[b,e], P. Bringel[c], J.R. Brown[k], F. Camera[l], S. Chmel[c], E. Clément[m], F.C.L. Crespi[l], C. Fahlander[d], A.B. Garnsworthy[e,n], A. Görgen[m], G. Hammond[o], M. Hellström[d], R. Hoischen[d], H. Honma[p], E.K. Johansson[d], A. Jungclaus[g], M. Kmieciek[f], W. Korten[m], A. Maj[f], S. Mandal[q], W. Meczynski[f], B. Million[l], A. Neußer[c], F. Nowacki[r], T. Otsuka[s,t], M. Pfützner[i], S. Pietri[e], Zs. Podolyák[e], A. Richard[a], M. Seidlitz[a], S.J. Steer[e], T. Striepling[a], T. Utsuno[s,t], J. Walker[g], N. Warr[a], C. Wheldon[u] and O. Wieland[l]

[a]*Institut für Kernphysik, Universität zu Köln, D-50937 Köln, Germany*
[b]*Gesellschaft für Schwerionenforschung, D-64291 Darmstadt, Germany*
[c]*Helmholtz-Institut für Strahlen- und Kernphysik, Universität Bonn, D-53115 Bonn, Germany*
[d]*Department of Physics, Lund University, S-22100 Lund, Sweden*
[e]*Department of Physics, University of Surrey, Guildford, GU2 7XH, UK*
[f]*The Henryk Niewodniczański Institute of Nuclear Physics, PL-31-342 Kraków, Poland*
[g]*Departamento de Física Teórica, Universidad Autonoma de Madrid, E-28049 Madrid, Spain*
[h]*Faculty of Physics, University of Sofia, BG-1164 Sofia, Bulgaria*
[i]*Institute of Experimental Physics, Warsaw University, PL-00-681 Warsaw, Poland*
[j]*Institute for Nuclear Research and Nuclear Energy, Bulgarian Academy of Sciences, BG-1784 Sofia, Bulgaria*
[k]*Department of Physics, University of York, York, Y01 5DD, UK*
[l]*Dipartimento di Fisica, Università di Milano, and INFN sezione di Milano, I-20133 Milano, Italy*
[m]*DAPNIA/SPhN, CEA Saclay, Gif-sur-Yvette, France*
[n]*WNSL, Yale University, New Haven, CT 06520-8124, USA*
[o]*School of Chemistry and Physics, Keele University, Staffordshire, ST5 5BG, UK*
[p]*University of Aizu, Fukushima 965-8580, Japan*
[q]*Department of Physics and Astrophysics, University of Delhi, Delhi - 110 007, India*
[r]*IReS, Université Louis Pasteur, Strasbourg, France*
[s]*Department of Physics and Center for Nuclear Study, University of Tokyo, Hongo, Tokyo 113-0033, Japan*
[t]*RIKEN, Hirosawa, Wako-shi, Saitama 351-0198, Japan*
[u]*Department SF7, Hahn-Meitner-Institut, D-14109 Berlin, Germany*

Abstract. The Rare Isotope Spectroscopic INvestigation at GSI (RISING) project is a major pan-European collaboration. Its physics aims are the studies of exotic nuclear matter with abnormal proton-to-neutron ratios compared with naturally occurring isotopes. RISING combines the FRagment Separator (FRS) which allows relativistic energies and projectile fragmentation reactions with EUROBALL Ge Cluster detectors for γ spectroscopic research. The RISING setup can be used in two different configurations. Either the nuclei of interest are investigated after being stopped or the heavy ions hit a secondary target at relativistic energies and the thereby occurring excitations are studied. For the latter case, MINIBALL Ge detectors and the HECTOR array are used in addition. Example achievements of the Fast Beam setup are presented and compared to various shell model calculations, while for the Stopped Beam setup initial results are shown.

Keywords: Gamma-ray spectroscopy; nuclear structure; excitation probabilities; nuclear isomers
PACS: 21.60.Cs; 23.20.Lv; 25.70.Mn

INTRODUCTION

One of the key issues in current nuclear structure physics research is the exploration of nuclei far away from the line of β-stability. This has led to the development of different techniques that permit the study of specific radioactive nuclei. In the case of projectile fragmentation or relativistic fission heavy ion beams are accelerated to an energy of up to 1 *A* GeV and then strike a thick target. Since this produces a vast number of different nuclei, the fragments of interest must be selected using their magnetic rigidity after the target, which is done at the FRS at GSI [1]. Here, two pairs of dipoles are used in the so called Bρ-ΔE-Bρ mode by placing a wedge-shaped aluminum degrader at the central focal plane of the FRS and setting the second pair of dipoles according to the energy loss of the sought-after fragments. The ions passing from the intermediate to the final focus of the FRS are identified on an event-by-event basis using their magnetic rigidity Bρ, their time of flight between two scintillation detectors, and their energy loss in a multi sampling ionization chamber.

RISING SETUP

When the heavy ions reach the final focus of the FRS, they can hit a secondary target, which enables the study of Coulomb excitation at relativistic energies or fragmentation processes towards even more exotic nuclei. Alternatively, they are implanted into a passive stopper followed by γ ray measurements of decays of isomeric states produced by the fragmentation or fission process in the primary target. This paper reports on initial and selected results of these two major RISING setups, the former being the Fast Beam setup [2], the latter being the Stopped Beam setup [3–5].

The Fast Beam Setup

In the Fast Beam setup relativistic Coulomb excitation and two-step fragmentation experiments were performed with energies in the range of 100 to 600 *A* MeV. A ^{197}Au reaction target with thicknesses from 0.4 to 2.0 g/cm^2 was used in the case of Coulomb

excitation, while two-step fragmentation experiments were carried out with a 0.7 g/cm^2 ^{9}Be target. The resulting reaction products were identified with respect to their charge and mass with the calorimeter telescope array CATE [6], consisting of 3 $\times$ 3 Si-CsI(Tl) modular ΔE-E telescopes mounted 1400 mm downstream of the target. For the proper Doppler correction, the position sensitive CATE Si detectors and an identical Si detector placed directly after the target served as tracking detectors. In the case of Coulomb excitation, unwanted nuclear contributions could be excluded by selecting sufficiently large impact parameters. This impact parameter could be obtained by tracking the heavy ions with position sensitive multiwire detectors upstream the target and the afore mentioned Si detectors.

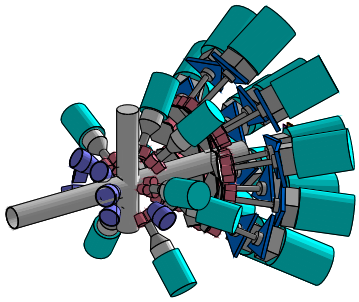

FIGURE 1. Drawing of the γ ray detector setup during the Fast Beam campaign. See text for details.

In order to measure γ rays emitted by excited states, the target area was surrounded by numerous detectors, as shown in Fig. 1: (i) 15 Cluster Ge detectors [7], positioned in three rings at extreme forward angles of 16°, 33°, and 36° at distances of 700 to 1400 mm, (ii) eight six-fold segmented MINIBALL triple Ge detectors [8] at distances of 200 to 400 mm, arranged in two rings with central angles of 51° and 85°, (iii) the HECTOR array [9, 10] at a distance of 300 mm, consisting of eight large volume BaF_2 detectors, situated at angles of 85° and 142°. In its least distance configuration, the efficiency for a γ ray of 1332 keV emitted from heavy ions at 100 A MeV was simulated to be 1.7% for the Cluster detectors, 3.8% for MINIBALL and 1.7% for HECTOR, not including add-back events.

The Stopped Beam Setup

The Stopped Beam setup can be used in two configurations to measure γ rays: Isomeric states produced in the fragmentation process are implanted into a passive stopper or heavy ions are implanted into an active β-sensitive stopper, thus enabling the search for excited states of exotic nuclei following β-decay. In contrast to the Fast Beam setup, a second degrader of variable thickness was put at the final focus of the FRS. This allowed the energy loss of the heavy ions to be tuned in such a way that the stopper could be kept at a moderate thickness.

The fifteen Ge Cluster detectors surrounding the stopper in the Stopped Beam setup are shown in Fig. 2. The Cluster detectors were placed in three rings of five detectors at angles of 51°, 90°, and 129° relative to the beam axis at a distance of approximately

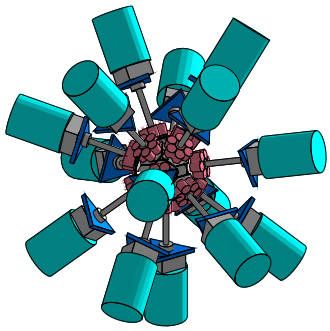

FIGURE 2. Drawing of the γ ray detector setup during the Stopped Beam campaign. See text for details.

22 cm from the center of the final focal plane of the FRS. The photopeak γ ray efficiency of the Stopped Beam Ge detector setup was measured to be 9(1)% at 1332 keV, not including add-back events [5]. Due to the high granularity of the Ge detector array of 105 crystals in total, a higher loss of efficiency was avoided after the prompt γ flash that was produced in the stopping process of the heavy ions. In order to identify the metastable states after the implantation, each γ ray was time stamped using a 40 MHz clock, which was part of the DGF4 timing and energy signal processing [11]. For both short-lived isomers and redundancy a conventional timing branch was installed in parallel and digitized with a short-range ($t \leq 1.0$ μs) and a long-range $t \leq 0.8$ ms VME TDC. This enabled the measurement of decays from isomeric states with half-lives in the region between several tens of ns up to 1 ms.

SELECTED EXPERIMENTAL RESULTS

Monopole Driven Shell Structure

During the Fast Beam campaign one of the key interests was the investigation of the monopole driven shell structure. This monopole part of the residual interaction controls the propagation of single particle energies with increasing occupation of a major shell. It causes a change of oscillator shell closures with magic numbers for very neutron rich nuclei of $N = 8, 20$ towards $N - 2 \times N_{HO} = 6, 16(14)$ [12, 13]. N_{HO} is the harmonic oscillator main quantum number . The weak $N = 40$ harmonic oscillator case should shift to a $N = 32, 34$ subshell closure, where the ambiguity for $N_{HO} > 1$ stems from the presence of j = 1/2 orbits which strongly mix with the neighboring higher-spin orbitals [13]. The monopole residual interaction is also expected to be of isospin symmetric nature, hence its effects can be studied by comparing the nuclear structure of the $N = 20$ isotones below ^{40}Ca with their $Z = 20$ mirror nuclei.

The RISING Fast Beam setup gives access to excitation energies $E_{2_1^+}$ of $I^\pi = 2_1^+$ and $B(E2; 2_1^+ \rightarrow 0^+)$ values that can both be used as signatures for shell structure. Two type of experiments were performed: A Coulomb excitation experiment of the neutron rich ^{54,56,58}Cr, which are located in between the $N = 40$ subshell closure across a deformed region to spherical nuclei at $N = 28$, second, and a two-step fragmentation

experiment to investigate the mirror energy difference, defined as $\Delta E_M = E_x(I, T_z = -T) - E_x(I, T_z = +T)$, between ^{36}Ca and ^{36}S.

The Subshell Closure at $N = 32, 34$ — Coulomb Excitation of ^{54,56,58}Cr

Experimentally, possible subshell closures may develop at $N = 32, 34$ in neutron rich Ca ($Z = 20$) isotopes as indicated by a rise in the 2_1^+ energy of ^{52}Ca [14]. The Ti and Cr ($Z = 22, 24$) isotopes exhibit a maximum of those energies at $N = 32$ [15–17].

Besides the 2_1^+ energies, $B(E2; 2_1^+ \rightarrow 0^+)$ values provide crucial information to test the evolution of subshell structures. Therefore, three experiments were performed to measure the Coulomb excitation of ^{54}Cr, ^{56}Cr and ^{58}Cr, where the known $B(E2; 2_1^+ \rightarrow 0^+)$ value in ^{54}Cr served as normalization and reference for possible systematic errors in the analysis.

A primary beam of ^{86}Kr with an energy of 480 A MeV was incident on a 2.5 g/cm^2 ^{9}Be target. Out of the fragmentation products, the Cr isotopes were selected and incident on a 1.0 g/cm^2 ^{197}Au target at energies of around 136 A MeV. More details of the experiment are given in Ref. [18]. The obtained Doppler corrected Cr spectra yield values of 8.7(30) W.u. for ^{56}Cr and 14.8(42) W.u. for ^{58}Cr. These results are shown in Fig. 3 together with the experimental $B(E2; 2_1^+ \rightarrow 0^+)$ and 2_1^+ systematics of the Ti and Cr isotopes and are compared to shell model calculations (KB3G, GXPF1, GXPF1A) [19–21].

The local peak in the $N = 32$ 2_1^+ energies is confirmed by a minimum of the $B(E2; 2_1^+ \rightarrow 0^+)$ values in the present experiment and a recent result for Ti isotopes [19]. For $N = 34$, however, the gap is not developed in Cr and Ti which leaves ^{54,56}Ca as

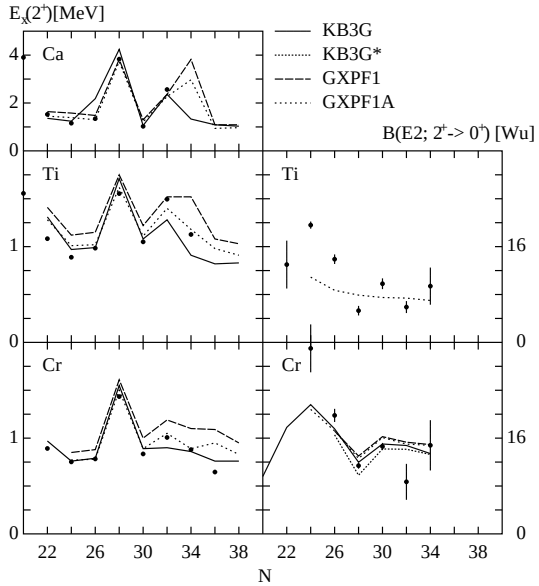

FIGURE 3. Experimental 2_1^+ energies and $B(E2; 2_1^+ \rightarrow 0^+)$ values of neutron rich Ca, Ti and Cr isotopes in comparison to different shell model calculations.

the crucial experimental probes. The shell model calculations reproduce the variation in the 2_1^+ energies but fail to reproduce the $B(E2;2_1^+ \rightarrow 0^+)$ values which stay almost unchanged in the different approaches from $N = 30$ to 34.

Mirror Symmetry in $A = 36$, $T = 2$ Nuclei

Going along the $N = 20$ isotones south of ^{40}Ca, the shell stabilization of ^{36}S, ^{34}Si and the shell quenching in ^{32}Mg are expected to be caused by the monopole part of the two-body interaction. This scenario is anticipated to be symmetric in isospin and may not or little affected by neutron binding energy differences [12, 13]. It can be verified in the $N = 20$ mirror region along the light Ca ($Z = 20$) isotopes. From the Ca isotopes, detailed spectroscopy exists only for ^{38}Ca [22], while no excited states are known for the $N = 16$ isotope, thus the mirror nucleus of ^{36}S is of high interest.

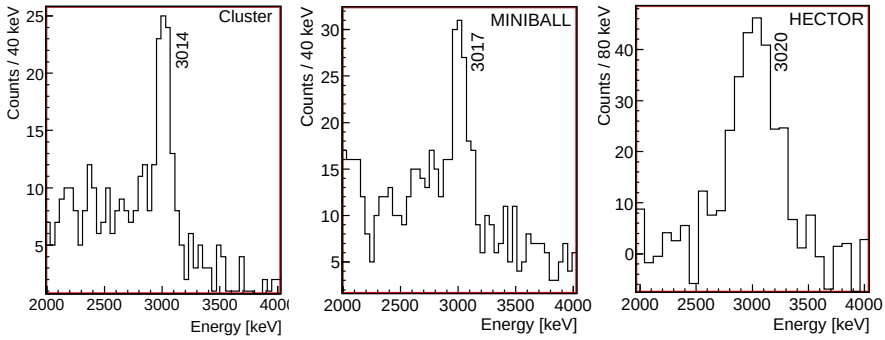

FIGURE 4. Doppler corrected ^{36}Ca gated γ ray spectra measured with the Cluster, MINIBALL and HECTOR detectors. For the HECTOR array the background was subtracted.

A beam of ^{40}Ca at an energy of 420 A MeV was bombarded on a 4.0 g/cm^2 ^{9}Be target. As a secondary beam ^{37}Ca was selected and incident on a 0.7 g/cm^2 ^{9}Be secondary target to populate excited states in ^{36}Ca. In Fig. 4 Doppler corrected γ ray spectra of ^{36}Ca are shown for the MINIBALL, Cluster and HECTOR detectors. The energy of the $2_1^+ \rightarrow 0^+$ transition was determined to 3015(16) keV, yielding a value of ΔE_M = –276(16) keV for the $A = 36$, $T = 2$ mirror pair. This value is significantly larger than mirror energy differences observed for $T = 1$ states in the *sd* and *pf* shell [15]. Other known $T = 2$ mirrors in the *sd* shell, $A = 24$ and 32, also exhibit much smaller mirror energy differences of –102(11) keV and –117(12) keV, respectively [23, 24].

In our approach to understand the large ΔE_M, we have used the experimental single-particle energies from the $A = 17$, $T = 1/2$ mirrors and applied these onto a modified isospin symmetric USD interaction [25, 26] in a shell model calculation. Monopole corrections were applied to reproduce the $Z, N = 14, 16$ shell gaps, the $I^\pi = 2_1^+$ excitation energies and the ^{40}Ca single hole energies. The results of this calculation are shown in Table 1 for ^{36}Ca and ^{36}S, yielding a value of ΔE_M = –268 keV. This is in close agreement to the experimental result and shows that the experimental single-particle energies may account empirically for the one-body part of Thomas-Ehrman and/or Coulomb effects [27, 28], since the isospin symmetry is preserved in the interactions' two-body matrix elements but not in the single-particle energies used.

TABLE 1. Comparison of shell model calculation with experimental values for ^{36}Ca and ^{36}S.

	$E_{2_1^+}$ **[keV]**		π**-gap [MeV]**		ν**-gap [MeV]**	
	Exp.*	**SM**†	**Exp.**	**SM**	**Exp.**	**SM**
^{36}Ca	3015(16)**	3290	4.55(30)		4.16(9)	3.999
^{36}S	3290.9(3)	3558	4.524(2)‡	4.244	5.585	

* From Ref. [15].
† Shell model calculation, see text for details.
** This work.
‡ Coulomb Corrected.

First Results from the Stopped Beam Setup

The Stopped Beam campaign started with the investigation of heavy odd-odd $N = Z$ nuclei along the proton drip-line [3]. It was followed by isomeric decay studies in the region of the doubly magic ^{56}Ni, ^{132}Sn and ^{208}Pb [29, 30]. We will focus on the results of ^{54}Ni, produced after the fragmentation of a ^{58}Ni primary beam, which demonstrate nicely the excellent possibilities of combining the FRS with the RISING γ ray spectrometer in its Stopped Beam configuration.

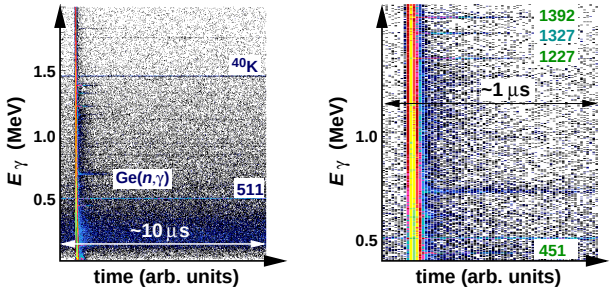

FIGURE 5. ^{54}Ni gated two-dimensional matrices of γ energy versus time after implantation.

After the identification of ^{54}Ni reaching the final focal plane with the FRS detectors, a correlation matrix between the γ energy and the time after the implantation can be generated. Two examples are shown in Fig. 5. On the left hand, a more general view provides an indication of the so-called prompt flash (vertical line), which marks the implantation time $t = 0$, as well as horizontal lines arising from, for example, room background or (n,γ) reactions in the Ge detectors. But more than that, also distinct and as a function of time fading horizontal lines are visible, indicating decays from isomeric states. Some of these are highlighted on the right hand side of Fig. 5, which zooms into the energy-time region of interest for ^{54}Ni. By setting cuts on distinct times after the implantation and comparing the intensities, information on the half-lives of the isomers can be obtained. Moreover, provided that the spectra are rich enough in statistics, $\gamma\gamma$ coincidence measurements can help to examine the level structure. This is done in Fig. 6 where in the upper background subtracted spectrum a simple projection of the two-dimensional panel is shown for the time range 0.05 μs $\leq t \leq$ 1.0 μs. In

this spectrum six discrete γ transitions at 146, 451, 1227, 1327, 1392, and 3241 keV are visible and all have a lifetime of $\tau \sim 220$ ns. In the lower panel, however, gates on the already established $6^+ \rightarrow 4^+ \rightarrow 2^+ \rightarrow 0^+$ cascade [31–33] are set at energies of 451, 1227, and 1392 keV. Since the lines observed at 146 and 3241 keV are clearly in coincidence with the cascade, they are suggested to be the $10^+ \rightarrow 8^+$ and $8^+ \rightarrow 6^+$ transitions [34], what also follows from the known mirror isomer ^{54}Fe [15]. Even a weak line at 3386 keV is visible, which can be associated to the small $10^+ \rightarrow 6^+$ $E4$ branch. The most surprising result is, however, that none of the observed γ rays comes in coincidence with the 1327 keV line, which is seen only in the singles spectrum. Since it has the same energy as the $9/2^- \rightarrow 7/2^-$ ground state transition in ^{53}Co, it is suggested that this $9/2^-$ state in ^{53}Co can be populated via a direct proton decay ($Q_p \sim 1.3$ MeV) from the isomeric state in ^{54}Ni [34].

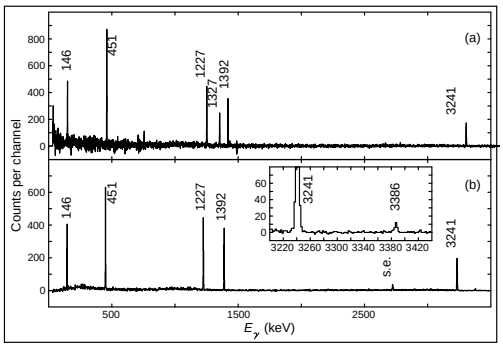

FIGURE 6. The upper panel (a) shows the background subtracted energy projection of the two-dimensional matrix of ^{54}Ni for the range $0.05\ \mu\text{s} \leq t \leq 1.0\ \mu\text{s}$. In the lower panel (b), the $\gamma\gamma$ coincidence with one of the transitions at 451, 1227, and 1392 keV demonstrates the correlation to other observed lines.

SUMMARY

The shown exemplary results demonstrate the possibilities of high resolution γ ray spectroscopy at relativistic energies utilizing the two-step fragmentation or Coulomb excitation technique with RISING, as has been shown for the results of ^{54,56,58}Cr and ^{36}Ca. A wealth of other interesting results have been obtained for example in relativistic Coulomb excitation of ^{108,112}Sn, ^{134}Ce, and ^{136}Nd [35, 36]. For the Stopped Beam campaign, a wide range of nuclei have been populated in isomeric states following fragmentation and fission: For example the long sought-after ^{82}Nb, ^{86}Tc, ^{130}Cd, and ^{204}Pt [29, 30, 37, 38]. Here, ^{54}Ni was chosen to illustrate the large capabilities of a highly efficient γ ray spectrometer used in combination with the FRS. In the future, a series of active stopper experiments is foreseen to perform β-delayed γ ray spectroscopy.

ACKNOWLEDGMENTS

The collaboration would like to thank the EUROBALL Owners Committee, the MINIBALL collaboration and the HECTOR collaboration for providing their γ detectors to

the RISING project. We also acknowledge the high beam intensities provided by the accelerator department at GSI. This permits us to study very exotic nuclei. This work is supported by the European Commission contract No. 506065 (EURONS), the German BMBF under grant Nos. 06BN-109, 06K-167, the Swedish Research Council, the Polish State Committee for Scientific Research (KBN grant No. 620/E-77/SPB/GSI/P-03/DWM105/2004-2007), the Bulgarian Science Fund under grant No. VUF06/05, and the EPRSC(UK).

REFERENCES

1. H. Geissel *et al.*, Nucl. Instr. Meth. B **70** (1992) 286.
2. H.J. Wollersheim *et al.*, Nucl. Instr. Meth. A **537** (2005) 637.
3. P.H. Regan *et al.*, Proc. of the NN06 conference, Nucl. Phys. **A**, in press.
4. S. Pietri *et al.*, Proc. of the CAARI'06 conference, to be published in Nucl. Inst. Meth. **B**.
5. S. Pietri *et al.*, Proc. of the 41st Zakopane School of Physics, to be published in Act. Phys. Pol. **B**.
6. R. Lozeva *et al.*, Nucl. Instr. Meth. A **562** (2006) 298.
7. J. Eberth *et al.*, Nucl. Inst. Meth. A **369** (1996) 135.
8. J. Eberth *et al.*, Prog. Part. Nucl. Phys. **46** (2001) 389.
9. A. Maj *et al.*, Nucl. Phys. A **571** (1994) 185.
10. F. Camera, Ph. D. Thesis, University of Milano, Italy, 1992.
11. M. Pfützner *et al.*, Nucl. Inst. Meth. A **493** (2002) 155.
12. T. Otsuka *et al.*, Phys. Rev. Lett. **87** (2001) 082502.
13. H. Grawe, Act. Phys. Pol. **B 34** (2003) 2267.
14. A. Huck *et al.*, Phys. Rev. **C 31** (1985) 2226.
15. ENSDF database, `http://www.nndc.bnl.gov/ensdf/`.
16. S.N. Liddick *et al.*, Phys. Rev. Lett. **92** (2004) 072502.
17. P.F. Mantica *et al.*, Phys. Rev. **C 67** (2003) 014311.
18. A. Bürger *et al.*, Phys. Lett. **B 622** (2005) 29.
19. D.C. Dinca *et al.*, Phys. Rev. **C 71** (2005) 041302.
20. E. Caurier *et al.*, Eur. Phys. J. **A 15** (2002) 145.
21. M. Honma *et al.*, Phys. Rev. **C 69** (2004) 034335.
22. P.D. Cottle *et al.*, Phys. Rev. **C 60** (1999) 031301.
23. S. Kanno *et al.*, Prog. Theor. Phys. (Kyoto), Suppl. **146** (2002) 575.
24. P.D. Cottle *et al.*, Phys. Rev. Lett. **88** (2002) 172502.
25. B.A. Brown, B.H. Wildenthal, Ann. Rev. of Nucl. Part. Sci. **38** (1988) 29.
26. Y. Utsuno *et al.*, Phys. Rev. **C 60** (1999) 054315.
27. R.G. Thomas, Phys. Rev. **88** (1952) 1109.
28. J.B. Ehrman, Phys. Rev. **81** (1951) 412.
29. M. Górska, A. Jungclaus, M. Pfützner *et al.*, to be published.
30. Zs. Podolyák *et al.*, Proc. of the RNB7 conference, to be published in Eur. Phys. J. **A**.
31. K.L. Yurkewicz *et al.*, Phys. Rev. C **70** (2004) 054319.
32. K. Yamada *et al.*, Eur. Phys. J. **A25** S1 (2005) 409.
33. A. Gadea *et al.*, Phys. Rev. Lett. **97** (2006) 152501.
34. D. Rudolph *et al.*, to be published.
35. A. Banu *et al.*, Phys. Rev. C **72** (2005) 061305(R).
36. T. Saito *et al.*, submitted to Phys. Rev. Lett.
37. L. Caceres *et al.*, Proc. of the 41st Zakopane School of Physics, to be published in Act. Phys. Pol. **B**.
38. A.B. Garnsworthy *et al.*, Proc. of the 41st Zakopane School of Physics, to be published in Act. Phys. Pol. **B**.